Euro. Jnl of Applied Mathematics (2004), *vol.* 15, *pp.* 651–677. © 2004 Cambridge University Press
doi:10.1017/S095679250400573X Printed in the United Kingdom

Evolution of a thin film of nematic liquid crystal with anisotropic surface energy

L. J. CUMMINGS

School of Mathematical Sciences, University of Nottingham, Nottingham NG7 2RD, UK
email: `linda.cummings@nottingham.ac.uk`

(*Received 5 January 2004; revised 15 September 2004*)

We use lubrication theory on the flow equations for nematic liquid crystals to derive a simple model describing the evolution of the film height under gravity, in the case of finite surface "anchoring energy" at the free surface and at the rigid substrate. This means that the molecules of the nematic have a preferred alignment at interfaces, modelled by a single-well potential surface energy (first introduced by Rapini & Papoular [9]). This paper generalises the earlier work of Ben Amar & Cummings, in which the orientation of the nematic liquid crystal molecules is effectively specified at both surfaces (strong anchoring; isotropic surface tension). Additional terms, analogous in some sense to Marangoni terms, are introduced into the PDE governing the film height evolution. The stability of the derived model is considered, and stability criteria are presented and discussed. The existence of static, drop-like solutions to the model is also briefly considered.

1 Introduction

In this paper we follow Ben Amar & Cummings [1] to derive a simple model, based on standard lubrication theory, describing the free boundary evolution of a thin film of nematic liquid crystal (NLC) on a rigid substrate. That paper assumed strong anchoring conditions on the director field $\boldsymbol{n}$ at both the rigid substrate and at the free surface of the film. Loosely speaking, the director field $\boldsymbol{n} = (\sin\theta\cos\phi, \sin\theta\sin\phi, \cos\theta)$ is a unit vector that gives the local preferred direction of the liquid crystal molecules; thus the strong anchoring condition amounts to saying that the orientation of the nematic liquid crystal molecules is effectively specified at interfaces. Here, we investigate the effect of finite anisotropic surface energy (in the form of finite anchoring strength for the azimuthal angle θ of the director), firstly at the free surface only, and secondly at both the free surface and the rigid substrate. We do this using the standard Rapini–Papoular [9] type formulae for the surface energy g

$$g = \gamma \pm \frac{A}{2}(\boldsymbol{n}\cdot\boldsymbol{p})^2.$$

The $(+)$ sign here corresponds to the (unit) vector $\boldsymbol{p}$ being the unfavoured director orientation, as any component of $\pm\boldsymbol{n}$ in the direction of $\boldsymbol{p}$ gives rise to an energy penalty. (The vectors $+\boldsymbol{n}$ and $-\boldsymbol{n}$ are considered equivalent in the theory.) The $(-)$ sign corresponds to $\boldsymbol{p}$ being the favoured orientation, since the surface energy is a minimum when $\boldsymbol{n}$ is parallel to $\boldsymbol{p}$. Both types of anchoring arise in practice, and both are considered in this paper. Strong anchoring corresponds to the limit $A \to \infty$.

The original study of Ben Amar & Cummings [1] was motivated by several experiments carried out by Cazabat *et al.* [2] at the Laboratoire de Physique de la Matiere Condensée du Collège de France, in which spontaneous fingering instabilities can be observed in such thin films, under certain circumstances. The basic physical set-up we consider is flow of a thin film of nematic liquid crystal, resting on a rigid substrate $z = 0$. The film height is given by $z = h(x, y, t)$, and gravity is assumed to be the only external force acting on the system.

2 Leslie–Ericksen equations

The details of the theory governing the flow of NLCs are beyond the scope of this paper, and we refer the reader elsewhere [3, 4, 7] for a discussion of the full model equations. The notation we employ is mostly the same as that used by Leslie [7], the two main functions being the velocity field of the flow, $\boldsymbol{v} = (v_1, v_2, v_3) = (u, v, w)$, and the director field $\boldsymbol{n}$, which is a unit vector describing the orientation of the anisotropic axis in the liquid crystal (the preferred direction of the liquid crystal molecules). Using standard tensor notation, and an over-dot to denote the usual convective derivative $\partial_t + \boldsymbol{v} \cdot \nabla$, the governing equations holding in the bulk sample, in the absence of any applied external fields (except gravity), are given by Leslie [7] as:

$$\sigma \ddot{n}_i = \lambda n_i - \frac{\partial W}{\partial n_i} + \left(\frac{\partial W}{\partial n_{i,j}}\right)_{,j} + \tilde{G}_i, \tag{2.1}$$

$$\rho \dot{v}_i + \sigma \ddot{n}_k n_{k,i} = -\pi_{,i} + \tilde{G}_k n_{k,i} + \tilde{t}_{ij,j}, \tag{2.2}$$

$$\nabla \cdot \boldsymbol{v} = 0. \tag{2.3}$$

Here, σ is an inertial constant; λ is a Lagrange multiplier ensuring that the director $\boldsymbol{n}$ is a unit vector; ρ is the constant density of the liquid crystal; W is the bulk elastic (Frank) energy, defined in terms of the director by

$$2W = K_1(\nabla \cdot \boldsymbol{n})^2 + K_2(\boldsymbol{n} \cdot \nabla \wedge \boldsymbol{n})^2 + K_3((\boldsymbol{n} \cdot \nabla)\boldsymbol{n}) \cdot ((\boldsymbol{n} \cdot \nabla)\boldsymbol{n}); \tag{2.4}$$

$$\tilde{G}_i = -\gamma_1 N_i - \gamma_2 e_{ik} n_k, \qquad e_{ij} = \frac{1}{2}\left(\frac{\partial v_i}{\partial x_j} + \frac{\partial v_j}{\partial x_i}\right); \tag{2.5}$$

$$N_i = \dot{n}_i - \omega_{ik} n_k, \qquad \omega_{ij} = \frac{1}{2}\left(\frac{\partial v_i}{\partial x_j} - \frac{\partial v_j}{\partial x_i}\right); \tag{2.6}$$

$$\pi = p + W + \psi_g, \tag{2.7}$$

where K_1, K_2, K_3, γ_1 and γ_2 are constants; p is the pressure and ψ_g is the gravitational potential (given, for instance, by $\rho g z$ or $\rho g x$, depending on the orientation of the sample). Finally, $\tilde{t}_{ij}$ is the extrastress tensor (related to the stress t_{ij} by $t_{ij} = -p\delta_{ij} + \tilde{t}_{ij}$), given by:

$$\tilde{t}_{ij} = \alpha_1 n_k n_p e_{kp} n_i n_j + \alpha_2 N_i n_j + \alpha_3 N_j n_i + \alpha_4 e_{ij} + \alpha_5 e_{ik} n_k n_j + \alpha_6 e_{jk} n_k n_i, \tag{2.8}$$

where the α_i are constant coefficients having the dimensions of viscosity[1] (though they are not necessarily positive), and $\mu := \alpha_4/2$ corresponds to the usual viscosity in the standard Newtonian (isotropic) case, when all other α_i are zero. The viscosities are related via the 'Onsager' relation

$$\alpha_2 + \alpha_3 = \alpha_6 - \alpha_5. \tag{2.9}$$

Equation (2.1) is the energy equation, in which the term in σ represents the rotational kinetic energy of the NLC molecules, the terms in W represent the elastic energy associated with the director field, and the $\tilde{G}$ term couples to the fluid flow. The three contributions to the elastic energy in (2.4) are known as splay, twist and bend, respectively, and represent energy penalties incurred when the director field has local behaviour of this kind. (See De Gennes & Prost [4] for further physical interpretation.)

Equation (2.2) is Newton's second law applied to the liquid crystal, the momentum equation for the flow, analogous in many ways to the Navier-Stokes equations, though with a much more complex stress tensor. Equation (2.3) represents incompressibility of the nematic liquid crystal.

2.1 Nondimensionalisation

Since we have a thin film, we make the usual lubrication theory scalings,

$$(x, y) = L(\tilde{x}, \tilde{y}),\ z = \delta L\tilde{z},\ u = U\tilde{u},\ v = U\tilde{v},\ w = \delta U\tilde{w},\ t = \frac{L}{U}\tilde{t},\ p = \frac{\mu U}{\delta^2 L}\tilde{p},$$

where L is the lengthscale of typical variations in the x- and y-directions, U is a typical flow speed; $\delta = h_0/L \ll 1$ is the aspect ratio of the film based on a typical film height h_0, and $\mu \equiv \alpha_4/2$ was chosen as the representative viscosity scaling in the pressure, since this corresponds to the usual viscosity in the isotropic case in (2.8). The coefficient α_4 is always positive, as may be shown by considering the entropy of the system [7]. If the free surface in the dimensional variables is given by $z = h(x, y, t)$ then we write $h = h_0\tilde{h}$, and in the dimensionless variables the free surface representation is $\tilde{z} = \tilde{h}(\tilde{x}, \tilde{y}, \tilde{t})$, with outward normal $\boldsymbol{v}^+$ given by

$$\boldsymbol{v}^+ = (-\delta\tilde{h}_{\tilde{x}}, -\delta\tilde{h}_{\tilde{y}}, 1)(1 + O(\delta^2)). \tag{2.10}$$

If $K = K_1$ is a representative value of the elastic constants K_1, K_2, K_3, (2.4) gives

$$W = O\left(\frac{K}{\delta^2 L^2}\right) \quad \Rightarrow \quad W = \frac{K}{\delta^2 L^2}\tilde{W}.$$

Henceforth we drop the tildes, on the understanding that we are working in the dimensionless variables (unless explicitly stated otherwise).

3 Strong anchoring at substrate

In this section we derive the governing equations for the case in which the anchoring at the rigid substrate is strong, but that at the free surface is relatively weak (finite anchoring

---

[1] In fact they are related to the γ_i in (2.5) by $\gamma_1 = \alpha_3 - \alpha_2$, $\gamma_2 = \alpha_6 - \alpha_5$, though we shall not need this.

strength). Since it is fairly simple experimentally to change the anchoring strength at a solid/nematic interface (and thus create a strongly anchoring surface if desired) by suitable treatment of the solid [4, 11], it is legitimate to do this. The case of finite anchoring strength at both boundaries is considered in § 4.

3.1 Energy

In the dimensionless variables equations (2.1) become

$$\begin{aligned}
\frac{\sigma\delta^2U^2}{K}\ddot{n}_1 &= \frac{\lambda\delta^2L^2}{K}n_1 - \left[\frac{\partial W}{\partial n_1} - \frac{\partial}{\partial x}\left(\frac{\partial W}{\partial n_{1x}}\right) - \frac{\partial}{\partial y}\left(\frac{\partial W}{\partial n_{1y}}\right) - \frac{\partial}{\partial z}\left(\frac{\partial W}{\partial n_{1z}}\right)\right]\\
&\quad + \frac{U\delta L}{2K}(\gamma_1-\gamma_2)u_zn_3 = 0,\\
\frac{\sigma\delta^2U^2}{K}\ddot{n}_2 &= \frac{\lambda\delta^2L^2}{K}n_2 - \left[\frac{\partial W}{\partial n_2} - \frac{\partial}{\partial x}\left(\frac{\partial W}{\partial n_{2x}}\right) - \frac{\partial}{\partial y}\left(\frac{\partial W}{\partial n_{2y}}\right) - \frac{\partial}{\partial z}\left(\frac{\partial W}{\partial n_{2z}}\right)\right]\\
&\quad + \frac{U\delta L}{2K}(\gamma_1-\gamma_2)v_zn_3 = 0,\\
\frac{\sigma\delta^2U^2}{K}\ddot{n}_3 &= \frac{\lambda\delta^2L^2}{K}n_3 - \left[\frac{\partial W}{\partial n_3} - \frac{\partial}{\partial x}\left(\frac{\partial W}{\partial n_{3x}}\right) - \frac{\partial}{\partial y}\left(\frac{\partial W}{\partial n_{3y}}\right) - \frac{\partial}{\partial z}\left(\frac{\partial W}{\partial n_{3z}}\right)\right]\\
&\quad - \frac{U\delta L}{2K}(\gamma_1+\gamma_2)(u_zn_1+v_zn_2) = 0.
\end{aligned}$$

Anticipating the velocity scale $U = O(\delta^3\rho gL^2/\mu)$ fixed by gravity acting perpendicular to the film driving the flow, we see that provided

$$\frac{\sigma\delta^8}{K}\left(\frac{\rho gL^2}{\mu}\right)^2 \ll 1, \qquad \frac{\delta^4\rho gL^3}{2K\mu}(\gamma_1\pm\gamma_2) \ll 1, \tag{3.1}$$

which should be the case for the $O(\mu\text{m})$-thickness films we consider, then the left-hand sides and each of the final terms on the right-hand sides of the above equations may be neglected, and (2.1) reduces to the appropriate *static* Euler-Lagrange equations for minimising the free energy of the film subject to the constraint $\boldsymbol{n}\cdot\boldsymbol{n} = 1$.[2] Our (slow) timescale is based on the fluid flow; we consider the regime in which the director configuration moves on a much faster timescale, so that the director ‘instantaneously’ adjusts to the fluid motion, and the director is thus always in its static equilibrium configuration.

Imposing the constraint $\boldsymbol{n}\cdot\boldsymbol{n} = 1$ directly we have

$$\boldsymbol{n} = (\sin\theta\cos\phi, \sin\theta\sin\phi, \cos\theta) \tag{3.2}$$

for some functions $\theta(x,y,z)$, $\phi(x,y,z)$, where ϕ is the azimuthal angle of the vector $\boldsymbol{n}$ about the axis $\theta = 0$; this enables us to eliminate the Lagrange multiplier λ in the Leslie formulation above. Making the simplifying assumption $K_1 = K_3 = K$ (the validity of this widely-used simplification is discussed by, for example, de Gennes & Prost [4, § 3.1.3.2]),

---

[2] Note though that if gravity instead acts parallel to the film the velocity scale is larger by a factor $1/\delta$, and the film must be correspondingly thinner for neglect of these terms.

the leading order elastic energy in the bulk is given by (2.4) as

$$2W = \theta_z^2 + \phi_z^2 \sin^2\theta + O(\delta). \tag{3.3}$$

The anisotropic surface energy enters only via the boundary conditions; to see how this arises it is instructive to carry out the free energy minimisation directly using a variational principle. Allowable director configurations are found at minima of the free energy, J, which is made up of contributions from the bulk, and from surface effects. We write

$$J = \iiint_{\Omega(t)} W \, dV + \iint_{\partial\Omega(t)} g \, dS, \tag{3.4}$$

where W is the leading order bulk elastic energy density defined in (3.3), g is the surface energy density, $\Omega(t)$ is the domain occupied by the liquid crystal sample, and $\partial\Omega(t)$ is the union of the free surface, $\partial\Omega^+(t)$, and the fixed interface $\partial\Omega^-$ at $z = 0$. The form of the surface energy, g, is chosen to mimic the fact that the NLC molecules at a boundary have a preferred direction (which depends on the properties of the boundary, and may be altered by treating the boundary). At the free interface we assume a Rapini–Papoular [9] formula for g, given in dimensional form by

$$g = \gamma_+ + \frac{A_+}{2}(\boldsymbol{n}\cdot\boldsymbol{\nu}^+)^2 = \gamma_+ + \frac{A_+}{2}\cos^2\theta + O(\delta), \tag{3.5}$$

where γ_+ is the isotropic contribution, and $\boldsymbol{\nu}^+$ is the normal to the free surface given by (2.10). Thus the surface energy is a minimum when the director lies in the plane of the free surface, and A_+ is the anchoring strength for this preferred configuration. This is known as planar anchoring, and is thought to be the situation holding at the free surface of certain nematic liquid crystals (e.g. PAA [4]). At the fixed interface $z = 0$ we shall for the moment assume strong anchoring, for simplicity: $\theta = 0$, and the director is forced to align perpendicular to the substrate (this is known as homeotropic anchoring; the angle ϕ is then arbitrary). The case of finite anchoring strength at this surface will be considered later.

We consider the variation induced in the energy J by small variations in the fields θ and ϕ:

$$\theta(x,y,z\,;t) \longmapsto \theta(x,y,z\,;t) + \epsilon\eta(x,y,z\,;t), \qquad \phi \longmapsto \phi(x,y,z\,;t) + \epsilon\lambda(x,y,z\,;t),$$

where $0 < \epsilon \ll 1$. Considering J as a functional of θ, θ_z and ϕ_z, in accordance with (3.4), (3.3) and (3.5), we may compute its first and second variations, that is, the order-ϵ and order-ϵ^2 terms in

$$\Delta J := J[\theta + \epsilon\eta, \theta_z + \epsilon\eta_z, \phi_z + \epsilon\lambda_z] - J[\theta, \theta_z, \phi_z].$$

We find, after applying the Divergence theorem,

$$\begin{aligned}\Delta J = {} & \epsilon \iiint_\Omega \eta\left(W_\theta - \left(W_{\theta_z}\right)_z\right) - \lambda\left(W_{\phi_z}\right)_z dV + \epsilon \iint_{\partial\Omega} \eta\left(g_\theta + \nu_3 W_{\theta_z}\right) + \lambda\nu_3 W_{\phi_z}\, dS \\ & + \frac{\epsilon^2}{2}\iiint_\Omega \eta^2\left(W_{\theta\theta} - \left(W_{\theta\theta_z}\right)_z\right) + \eta_z^2 W_{\theta_z\theta_z} + \lambda_z^2 W_{\phi_z\phi_z} + 2\eta\lambda_z W_{\theta\phi_z} + 2\eta_z\lambda_z W_{\theta_z\phi_z}\, dV \\ & + \frac{\epsilon^2}{2}\iint_{\partial\Omega} \eta^2\left(g_{\theta\theta} + \nu_3 W_{\theta\theta_z}\right) dS + O(\epsilon^3),\end{aligned} \tag{3.6}$$

where $v_3 = \pm 1$ (the z-component of the vector $\boldsymbol{v}^{\pm}$ normal to the upper/lower surface of the film, in the direction away from the fluid).

The first variation must vanish at a minimum, for all admissible variations η and λ. (The second variation tells us whether or not we have an energy minimum, and hence whether or not the solution is stable, and will be used later.) Hence using (3.3), the volume integral at order ϵ gives

$$\theta_{zz} = \frac{\phi_z^2}{2} \sin 2\theta \quad \text{in } \Omega, \tag{3.7}$$

$$\left(\phi_z \sin^2 \theta\right)_z = 0 \quad \text{in } \Omega, \tag{3.8}$$

while the surface integral at this order tells us that (1) *either* η must vanish at the boundary, i.e. θ is specified at the boundary (a strong anchoring condition on θ); *or*

$$g_\theta \pm \theta_z = 0 \quad \text{on } \partial\Omega^{\pm}, \tag{3.9}$$

and (2) *either* λ must vanish at the boundary, i.e. ϕ is specified at the boundary (a strong anchoring condition on ϕ); *or*

$$\phi_z \sin^2 \theta = 0 \quad \text{on } \partial\Omega^{\pm} \tag{3.10}$$

(a 'natural' boundary condition on ϕ). A discussion of possible boundary conditions at nematic/isotropic interfaces is given in De Gennes & Prost [4, § 3.1.4]. As outlined above, we shall assume strong anchoring of θ at the rigid substrate (such conditions may be created by suitable treatment of the bounding surface, e.g. rubbing or etching), and finite surface energy defined by (3.5) at the free surface. Unless strong anchoring on the twist angle ϕ is imposed (which is not anticipated at a free interface, and in any case is not consistent with the assumed form for the surface energy g) it is immediate from (3.8) and (3.10) that $\phi_z \sin^2 \theta = 0$ throughout Ω, and so, unless θ is a multiple of π throughout the sample, ϕ must be constant everywhere. We thus set

$$\phi \equiv 0 \tag{3.11}$$

throughout the sample without loss of generality, and the director field is effectively two-dimensional within the validity of our model. However, this does not preclude two-dimensional disturbances to the film height.

Since we impose strong anchoring $\theta = 0$ at $z = 0$, to leading order the solution for the director angle θ is

$$\theta = a(x, y, t)z. \tag{3.12}$$

Thus, ah represents the total angle turned through by the director across the sample. To satisfy the free surface condition (3.9) $a(x, y, t)$ satisfies

$$a(x, y, t) = \frac{\mathscr{A}_+}{2} \sin\left[2a(x, y, t)h(x, y, t)\right], \tag{3.13}$$

where the dimensionless anchoring strength $\mathscr{A}_+ = \delta L A_+ / K$. Nontrivial solutions of (3.13) exist only if $\mathscr{A}_+ h > 1$ everywhere; if this is the case then there may be multiple solutions of (3.13) (see Figure 1). Solutions a may be found in terms of h by considering the intersections of the curves $y = 2ah/(\mathscr{A}_+ h)$ and $y = \sin 2ah$. In the case that multiple

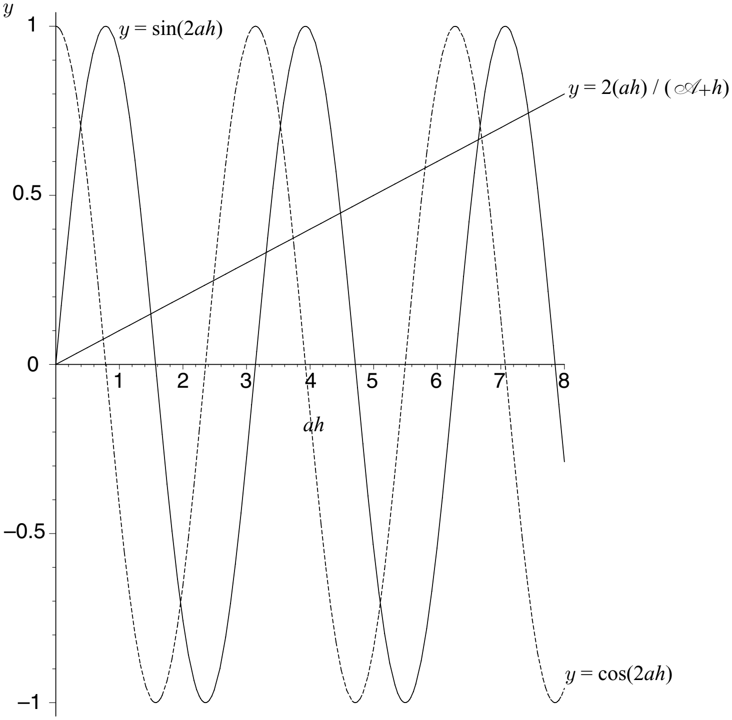

FIGURE 1. Solutions a are given by the intersection of the solid curves $y = \sin(2ah)$ and $y = 2(ah)/(\mathscr{A}_+h)$, and these are stable if the corresponding value of $\cos(2ah)$ (the dotted curve) is negative. Thus, the first (trivial) root is unstable, the second stable (provided it lies in $ah > \pi/4$), the third unstable, and so on, nontrivial solutions alternating between stable and unstable as a increases for as long as roots exist.

solutions exist, not all will be stable. By considering the sign of the second variation in (3.6), given by

$$(\Delta J)_2 = \frac{\epsilon^2}{2}\iiint_{\Omega} \eta_z^2 dV - \frac{\epsilon^2 \mathscr{A}_+}{2}\iint_{\partial\Omega^+} \eta^2 \cos 2ah\, dS, \tag{3.14}$$

it may be deduced that roots for which $\cos(2ah) < 0$ are stable (small variations in the solution only increase the energy), while those for which $\cos(2ah) > 0$ are unstable. Hence, considering Figure 1, only if $\mathscr{A}_+h > \pi/2$ everywhere will stable solutions for a exist. The stable configuration observed in experiments will correspond to the smallest (positive, without loss of generality) nontrivial root of (3.13), as this is the lowest energy state (recall that ah represents the angle the director turns through across the film). Thus, when nontrivial solutions exist, the observed solution will be such that

$$\frac{\pi}{4h} < a < \frac{\pi}{2h}. \tag{3.15}$$

The free elastic energy W is then given by

$$W = \frac{\theta_z^2}{2} = \frac{a(x, y, t)^2}{2}. \tag{3.16}$$

3.2 Momentum

3.2.1 *Gravity perpendicular to the film*

We turn now to the momentum equations (2.2), considering first the case in which gravity acts in the z-direction. Looking at the x- and y-components, the dominant balance of terms must be such that, in the original dimensional variables,

$$\frac{\partial \pi}{\partial x} \sim \frac{\partial \tilde{t}_{13}}{\partial z}, \quad \frac{\partial \pi}{\partial y} \sim \frac{\partial \tilde{t}_{23}}{\partial z},$$

and examination of the dominant terms in π, $\tilde{t}_{13}$ and $\tilde{t}_{23}$ gives the leading order equations in the dimensionless variables as

$$\frac{\partial p}{\partial x} + \mathscr{N}\frac{\partial W}{\partial x} = \frac{\partial}{\partial z}\left\{\frac{\partial u}{\partial z}\left(2\alpha_1 \sin^2\theta\cos^2\theta + (\alpha_5-\alpha_2)\cos^2\theta + (\alpha_3+\alpha_6)\sin^2\theta + 1\right)\right\} \quad (3.17)$$

$$\frac{\partial p}{\partial y} + \mathscr{N}\frac{\partial W}{\partial y} = \frac{\partial}{\partial z}\left\{\frac{\partial v}{\partial z}\left((\alpha_5-\alpha_2)\cos^2\theta + 1\right)\right\}. \quad (3.18)$$

Here the dimensionless parameter $\mathscr{N}$ is defined by $\mathscr{N} = K/(\mu U L)$, and is the inverse Ericksen number. The α_i are now normalised by division by $\alpha_4 = 2\mu$. Note that if $\alpha_i = 0$ $(i \mp 4)$ and $\mathscr{N} = 0$ (zero Frank elastic energy), which is the case for a Newtonian fluid, then (3.17) and (3.18) reduce to the standard Newtonian thin film equations (for example, see Myers [8]).

The z-component of (2.2) gives

$$0 = \frac{\partial p}{\partial z} + \mathscr{B} \quad (3.19)$$

at leading order (W, as given by (3.3), (3.11) and (3.12) is independent of z), where the Bond number $\mathscr{B} = \delta^3\rho g L^2/(\mu U)$. If gravity is the driving force, we fix the velocity scale $U = \delta^3\rho g L^2/\mu$. As in Newtonian flows with surface tension gradients (Marangoni flows), we assume that the normal component of the stress vector at the free surface balances surface tension times curvature, and that the in-plane component of the stress vector is balanced by surface tension (or surface energy) gradients in the plane of the surface. With the stress tensor $t_{ij} = -p\delta_{ij} + \tilde{t}_{ij}$ this yields the leading order boundary conditions:

$$p = -\mathscr{C}\left(\frac{\partial^2 h}{\partial x^2} + \frac{\partial^2 h}{\partial y^2}\right) \quad \text{on } y = h(x,y,t), \quad (3.20)$$

$$\begin{aligned}&\frac{\partial u}{\partial z}\left(2\alpha_1 \sin^2\theta\cos^2\theta + (\alpha_5-\alpha_2)\cos^2\theta + (\alpha_3+\alpha_6)\sin^2\theta + 1\right)\\ &\quad = -\mathscr{A}_{+}\mathscr{N}\frac{\partial a}{\partial x}h\sin\theta\cos\theta = -\mathscr{N}ha\frac{\partial a}{\partial x} \quad \text{on } y = h(x,y,t),\end{aligned} \quad (3.21)$$

$$\begin{aligned}\frac{\partial v}{\partial z}\left((\alpha_5-\alpha_2)\cos^2\theta + 1\right) &= -\mathscr{A}_{+}\mathscr{N}\frac{\partial a}{\partial y}h\sin\theta\cos\theta\\ &= -\mathscr{N}ha\frac{\partial a}{\partial y} \quad \text{on } y = h(x,y,t),\end{aligned} \quad (3.22)$$

((3.13) was used to simplify the right-hand sides of (3.21) and (3.22)), where the inverse capillary number $\mathscr{C} = \delta^3\gamma_+/(\mu U)$. We also impose no slip on $z = 0$:

$$u = v = 0 \quad \text{on } z = 0,$$

and a kinematic boundary condition

$$w = \frac{\partial h}{\partial t} + u\frac{\partial h}{\partial x} + v\frac{\partial h}{\partial y}, \qquad \text{on } z = h(x, y, t),$$

which, taken together with (2.3), gives conservation of flux,

$$\frac{\partial h}{\partial t} + \frac{\partial}{\partial x}\left(\int_0^{h(x,y,t)} u\,dz\right) + \frac{\partial}{\partial y}\left(\int_0^{h(x,y,t)} v\,dz\right) = 0. \tag{3.23}$$

One can then solve (3.19) for p, substitute in (3.17) and (3.18) to solve for u_z and v_z using the boundary conditions derived above, and, using the relations

$$\int_0^h u\,dz = \int_0^h u_s(h - s)\,ds, \qquad \int_0^h v\,dz = \int_0^h v_s(h - s)\,ds,$$

finally substitute the results into (3.23) to obtain a partial differential equation governing the evolution of the film height:

$$\begin{aligned}\frac{\partial h}{\partial t} + \frac{\partial}{\partial x}&\left[\left(\mathscr{C}\left(\nabla^2 h\right)_x - \mathscr{B}h_x - \mathscr{N}aa_x\right)\mathscr{I}_1 - \mathscr{N}haa_x\mathscr{I}_2\right] \\ &+ \frac{\partial}{\partial y}\left[\left(\mathscr{C}\left(\nabla^2 h\right)_y - \mathscr{B}h_y - \mathscr{N}aa_y\right)\mathscr{I}_3 - \mathscr{N}haa_y\mathscr{I}_4\right] = 0\end{aligned} \tag{3.24}$$

where, recall, h and a are related by (3.13), subject to the restriction (3.15), and $\mathscr{I}_1$ to $\mathscr{I}_4$ are defined by:

$$\mathscr{I}_1 = \frac{F_1(2ah)}{a^3},\ \mathscr{I}_2 = \frac{F_2(2ah)}{a^2},\ \mathscr{I}_3 = \frac{F_3(2ah)}{a^3},\ \mathscr{I}_4 = \frac{F_4(2ah)}{a^2}, \tag{3.25}$$

where

$$\begin{aligned}F_1(\lambda) &= \frac{1}{4}\int_0^\lambda \frac{(\lambda - \xi)^2\,d\xi}{\alpha_1\sin^2\xi + 2\eta_b(1 - \cos\xi) + 2\eta_c(1 + \cos\xi)} \\ F_2(\lambda) &= \frac{1}{2}\int_0^\lambda \frac{(\lambda - \xi)\,d\xi}{\alpha_1\sin^2\xi + 2\eta_b(1 - \cos\xi) + 2\eta_c(1 + \cos\xi)} \\ F_3(\lambda) &= \frac{1}{4}\int_0^\lambda \frac{(\lambda - \xi)^2\,d\xi}{2\eta_c(1 + \cos\xi) + (1 - \cos\xi)} \\ F_4(\lambda) &= \frac{1}{2}\int_0^\lambda \frac{(\lambda - \xi)\,d\xi}{2\eta_c(1 + \cos\xi) + (1 - \cos\xi)}.\end{aligned}$$

Here the Miesowicz viscosities η_b and η_c are defined by [4]

$$\eta_b = \frac{1}{2}(1 + \alpha_3 + \alpha_6), \quad \eta_c = \frac{1}{2}(1 - \alpha_2 + \alpha_5), \tag{3.26}$$

and the Onsager relation (2.9) was used in simplifying the expressions. These viscosities η_b and η_c are real physical viscosities, and hence are positive. It is thus clear that $F_3(\lambda)$ and $F_4(\lambda)$ are positive for $\lambda > 0$, and hence that $\mathscr{I}_3 > 0$ and $\mathscr{I}_4 > 0$. Whilst the signs of

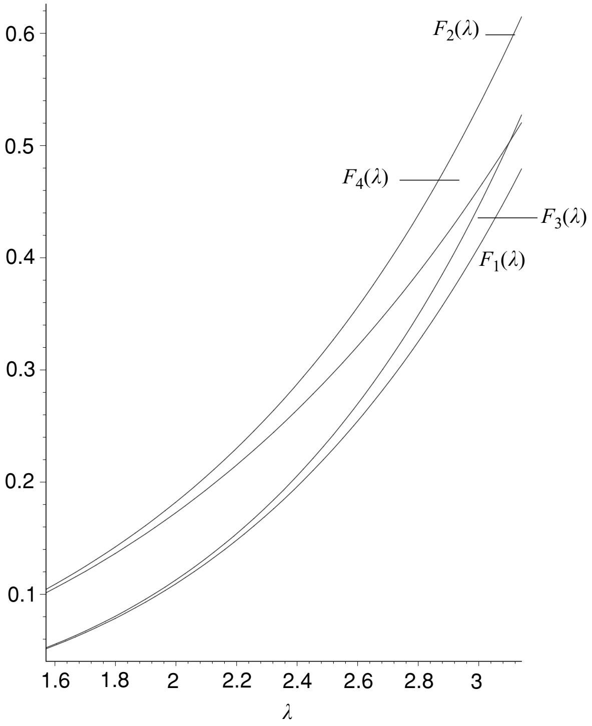

FIGURE 2. The functions $F_i(\lambda)$ for $\pi/2 < \lambda < \pi$, using the values for the viscosities α_i of MBBA at 25°C given in Kneppe *et al.* [6].

$\mathscr{I}_1$ and $\mathscr{I}_2$ are not immediately obvious, we would at least anticipate $\mathscr{I}_1 > 0$, given the form of the governing equation (3.24).

For the liquid crystal MBBA in the nematic state at 25°C, the values for the viscosities provided by Kneppe *et al.* (Table I) [6] yield $\alpha_1 = -0.2191$, $\alpha_2 = -1.3365$, $\alpha_3 = -0.0133$, $\alpha_5 = 0.9431$ $\alpha_6 = -0.4068$ for the normalised viscosities. In this case the functions $F_i(\lambda)$ are all positive. They are sketched in figure 2, for $\pi/2 < \lambda < \pi$, which, by (3.15), is the range of interest. Thus the $\mathscr{I}_i$ are all positive for MBBA.

Note that the film thickness h cannot go to zero within the framework of this model, since for sufficiently small thicknesses h no stable energy minima will exist (the stable roots a all disappear; see Figure 1). Hence we are restricted to considering films sufficiently thick that stable energy minima exist.

3.2.2 *Gravity parallel to the film*

When gravity in the $(-x)$-direction is assumed to be the driving mechanism, which is equivalent to a flow driven by a constant influx supplied at $x = +\infty$, (3.19) is replaced by $p_z = 0$, and (3.17) is modified with an extra gravity term $(-\mathscr{B}_1)$ on the right-hand side, where $\mathscr{B}_1 = \mathscr{B}/\delta$. An analogous procedure then leads to

$$\begin{aligned}\frac{\partial h}{\partial t} + \frac{\partial}{\partial x}\left[\left(\mathscr{C}\left(\nabla^2 h\right)_x - \mathscr{B}_1 - \mathscr{N} a a_x\right)\mathscr{I}_1 - \mathscr{N} h a a_x \mathscr{I}_2\right]\\ + \frac{\partial}{\partial y}\left[\left(\mathscr{C}\left(\nabla^2 h\right)_y - \mathscr{N} a a_y\right)\mathscr{I}_3 - \mathscr{N} h a a_y \mathscr{I}_4\right] = 0. \qquad (3.27)\end{aligned}$$

Note that if the gravity is the driving mechanism, then the velocity scale here is fixed by setting $\mathscr{B}_1 = 1$, giving a velocity scale a factor of $1/\delta$ larger than in the preceding case.

3.3 Limiting cases of the governing equations

Newtonian fluid

With $\alpha_1 = \alpha_2 = \alpha_3 = \alpha_5 = \alpha_6 = 0$ it is easily verified that

$$\mathscr{I}_1 = \mathscr{I}_3 = \frac{h^3}{3}, \quad \text{and} \quad \mathscr{I}_2 = \mathscr{I}_4 = \frac{h^2}{2}.$$

If we also take $\mathscr{N} = 0$ (which is the case if the Frank energy coefficient K is zero, as is the case for a Newtonian fluid), then equations (3.24) and (3.27) are standard, and have been widely studied. The review article by Myers [8] gives an overview of lubrication-type equations, and many related references.

$\mathscr{A}_+ \to \infty$, strong anchoring

This is the case previously studied by Ben Amar & Cummings. In this case the function a determined by (3.13) approaches $\pi/(2h)$ as

$$a \sim \frac{\pi}{2h}\left(1 - \frac{1}{\mathscr{A}_+ h} + \cdots\right),$$

so $\mathscr{I}_1 \to F_1(\pi)/a^3 = k_1h^3$, $\mathscr{I}_2 \to F_2(\pi)/a^2 = k_2h^2$, $\mathscr{I}_3 \to F_3(\pi)/a^3 = k_3h^3$, $\mathscr{I}_4 \to F_4(\pi)/a^2 = k_4h^2$, for some positive constants k_1-k_4. In this case equation (3.24) reduces to

$$\begin{aligned}\frac{\partial h}{\partial t} &+ \frac{\partial}{\partial x}\left[k_1h^3\left(\mathscr{C}(\nabla^2 h)_x - \mathscr{B}h_x\right) + \tilde{\mathscr{N}}h_x(k_1+k_2)\right] \\ &+ \frac{\partial}{\partial y}\left[k_3h^3\left(\mathscr{C}(\nabla^2 h)_y - \mathscr{B}h_y\right) + \tilde{\mathscr{N}}h_y(k_3+k_4)\right] = 0, \qquad (3.28)\end{aligned}$$

where $\tilde{\mathscr{N}} = \mathscr{N}\pi^2/4$, and (3.27) reduces to

$$\begin{aligned}\frac{\partial h}{\partial t} &+ \frac{\partial}{\partial x}\left[k_1h^3\left(\mathscr{C}(\nabla^2 h)_x - \mathscr{B}_1\right) + \tilde{\mathscr{N}}h_x(k_1+k_2)\right] \\ &+ \frac{\partial}{\partial y}\left[k_3h^3\left(\mathscr{C}(\nabla^2 h)_y\right) + \tilde{\mathscr{N}}h_y(k_3+k_4)\right] = 0. \qquad (3.29)\end{aligned}$$

The one-dimensional version of these equations is equivalent to that given in Ben Amar & Cummings [1] (redefine $\mathscr{N}$ and rescale time appropriately, as was done there), but the two-dimensional versions given above are different, as the naive two-dimensional generalisation assumed in Ben Amar & Cummings [1] does not in fact hold. The above equations are the correct two-dimensional version when there is strong anchoring at the free surface. Flows driven both by gravity parallel to the film, and by gravity perpendicular to the film, were considered in Ben Amar & Cummings [1], instabilities being found in both cases.

3.4 Analysis of gravity-spreading case

We focus now on the case of § 3.2.1, in which gravity acts perpendicular to the film. There are two possible experimental situations: either partial or total wetting, according as the 'spreading power' of the liquid crystal/substrate system is negative or positive [5]. We mostly consider the case of total wetting in this paper, to avoid the delicate issue of contact lines.

3.4.1 *Stability analysis of flat film*

In the totally wetting case, in the absence of instability, we expect the drop to continue spreading indefinitely, the ultimate state being a monolayer. For small drops spreading under gravity, if the Bond number is unity, the timescale of the spreading is very long, $L/U = \mu/(\delta^3 \rho g L) \gg 1$, so the spreading occurs slowly; however after some time the initial drop will have flattened considerably.

Taking into account this flattening, and the slow timescale of the spreading, we simplify the problem by considering the stability of the simplest static solution to the equation (3.24): the flat profile $h \equiv 1$. We perturb this solution, writing

$$\begin{aligned} h(x,y,t) &= 1 + \epsilon e^{\beta t} h_1(x,y) + O(\epsilon^2), \\ a(x,y,t) &= a_0 + \epsilon e^{\beta t} a_1(x,y) + O(\epsilon^2), \end{aligned}$$

where, in line with the observations after (3.13), and the inequalities (3.15), a_0 is the solution of

$$2a_0 = \mathscr{A}_+ \sin 2a_0, \quad \frac{\pi}{4} < a < \frac{\pi}{2}.$$

Since the solutions a and h must both more generally satisfy (3.13), it follows that a_1 and h_1 are related by

$$a_1 = -\frac{a_0 h_1 \sqrt{\mathscr{A}_+^2 - 4a_0^2}}{1 + \sqrt{\mathscr{A}_+^2 - 4a_0^2}} = -\lambda h_1 \tag{3.30}$$

(the restriction $\mathscr{A}_+ > 2a_0$ is necessary for the solution a_0 to exist), where the second equality defines the positive constant λ. Substitution in (3.24) gives the eigenvalue problem for h_1

$$\begin{aligned} &\beta h_1 + \mathscr{I}_1 \frac{\partial}{\partial x}\left[\mathscr{C}\left(\nabla^2 h_1\right)_x - \mathscr{B} h_{1x}\right] + \mathscr{N} a_0 \lambda h_{1xx}(\mathscr{I}_1 + \mathscr{I}_2) + \\ &\mathscr{I}_3 \frac{\partial}{\partial y}\left[\mathscr{C}\left(\nabla^2 h_1\right)_y - \mathscr{B} h_{1y}\right] + \mathscr{N} a_0 \lambda h_{1yy}(\mathscr{I}_3 + \mathscr{I}_4) = 0, \end{aligned}$$

where the $\mathscr{I}_i$ are evaluated at the leading-order solution $a = a_0$, $h = 1$. Bounded solutions to this equation are (up to constant multiples) of the form $h_1(x,y) = \exp(ikx + iqy)$ for k, $q \in \mathbb{R}$. Thus the dispersion relation between β and the wavenumbers (k,q) is:

$$\beta(k,q) = -[\mathscr{I}_1 k^2 + \mathscr{I}_3 q^2](\mathscr{C}(k^2 + q^2) + \mathscr{B} - \mathscr{N} a_0 \lambda) + \mathscr{N} a_0 \lambda [\mathscr{I}_2 k^2 + \mathscr{I}_4 q^2],$$

and the general solution to this order is of the form

$$h(x, y, t) = 1 + \epsilon \int_{-\infty}^{\infty} \int_{-\infty}^{\infty} A(k, q) e^{\beta(k,q)t} e^{ikx} e^{iqy} \, dk \, dq.$$

Clearly, assuming the $\mathscr{I}_i$ are positive (which we have seen is the case for the liquid crystal MBBA in the nematic state), then depending on the relative sizes of $\mathscr{B}$ and $\mathscr{N}$ there is a range of positive eigenvalues $\beta(k, q)$ for small wavenumbers (the capillary terms are then negligible), hence for $\mathscr{N}$ sufficiently large the film will be unstable to small wavenumber perturbations.

From the definitions of $\mathscr{N}$ and $\mathscr{B}$ we see that

$$\frac{\mathscr{N}}{\mathscr{B}} = \frac{K}{\rho g (\delta L)^3}.$$

The factor (δL) in the denominator is the representative thickness of the droplet, h^* say, which decreases as the droplet spreads. The ratio $\mathscr{N}/\mathscr{B}$ thus inevitably increases as the spreading progresses, and, if it exceeds the critical value required to give a range of positive eigenvalues then instability will set in. We conclude that when the anchoring strength at the free surface is finite, with strong anchoring at the substrate, a sufficiently thin film will destabilise spontaneously. This result is in line with the strong anchoring result of Ben Amar & Cummings [1].

Physically, as the film gets thinner, the director is still required to bend through some finite angle across it, and this becomes more and more difficult to achieve. Ultimately, it is preferable for the film to change the orientation of its free surface, giving the instability. In the extreme case of strong anchoring at both surfaces, the director is forced to bend through a constant angle, irrespective of the thickness of the film. With finite surface energy there is some leeway in the angle the director must turn through; roughly speaking, the lower the value of the surface energy, the smaller the angle that the director must bend through, and the thinner a film can be sustained stably.

4 Finite surface energy at substrate

We now derive the governing equations for the case in which the anchoring strength at the solid substrate and at the free surface are both finite.

4.1 Energy: Finite homeotropic anchoring at substrate and finite planar anchoring at free surface

The surface energy at the free surface is again given by (3.5) (planar anchoring of finite anchoring strength), and as before we assume homeotropic anchoring at the solid substrate, but now of finite anchoring strength A_-, so that the surface energy at this surface is given by

$$g = \gamma_- - \frac{A_-}{2} (\boldsymbol{n} \cdot \boldsymbol{v}_-)^2 = \gamma_- - \frac{A_-}{2} \cos^2 \theta. \tag{4.1}$$

One may again carry out the variational process, obtaining equations (3.6)–(3.10) exactly as before. Now, however, we do not impose the value of θ on $z = 0$, but fix it by (3.9).

With the same assumptions as before we again obtain $\phi \equiv 0$ without loss of generality, and the director angle θ is then given by

$$\theta = a(x, y, t)z + b(x, y, t), \tag{4.2}$$

where to satisfy the boundary conditions (3.9) at each interface a and b must satisfy

$$a = \frac{\mathscr{A}_+}{2}\sin(2ah + 2b), \tag{4.3}$$

$$a = \frac{\mathscr{A}_-}{2}\sin(2b). \tag{4.4}$$

Clearly $a \equiv 0$, $b = 0, \pi/2$ are possible solutions (these are the only possible solutions with $a = 0$, because two solutions in which a is the same and b differs only by an integer multiple of π, are equivalent).

To enable further analytical progress with the nontrivial solutions, we make the simplifying assumption that the two anchoring strengths $\mathscr{A}_+$ and $\mathscr{A}_-$ are equal (this is in the same spirit as the equal-elastic-constants assumption made earlier in § 2.1):

$$\mathscr{A}_+ = \mathscr{A}_- = \mathscr{A}. \tag{4.5}$$

Then, combining equations (4.3) and (4.4), we find that possible solutions must satisfy

$$(1) \quad \sin(ah) = 0, \quad \text{or } (2) \quad \cos(ah + 2b) = 0. \tag{4.6}$$

Stability of these solutions is determined by the sign of the second variation, which from (3.6) has the form

$$\begin{aligned}(\Delta J)_2 = \frac{\epsilon^2}{2}\iiint_\Omega \eta_z^2 dV - \frac{\mathscr{A}\epsilon^2}{2}\iint_{\partial\Omega^+}\eta^2\cos(2ah + 2b)dS \\ + \frac{\mathscr{A}\epsilon^2}{2}\iint_{\partial\Omega^-}\eta^2\cos(2b)dS.\end{aligned} \tag{4.7}$$

Case (1): $\sin(ah) = 0$

Here, $ah = n\pi$ for integers n (which may be assumed positive without loss of generality), and there are two relevant solutions for b for each n:

$$b = \frac{1}{2}\mathrm{Sin}^{-1}\left(\frac{2n\pi}{\mathscr{A}h}\right), \quad b = \frac{\pi}{2} - \frac{1}{2}\mathrm{Sin}^{-1}\left(\frac{2n\pi}{\mathscr{A}h}\right),$$

where Sin^{-1} denotes the principal branch of the inverse sine function. Clearly, these solutions exist only if $2n\pi/(\mathscr{A}h) \leqslant 1$. If they exist, then

$$\cos(2ah + 2b) = \cos(2b + 2n\pi) = \cos(2b).$$

Hence in the 2nd variation (4.7), whatever the sign of $\cos(2b)$, there is always one positive surface contribution and one negative surface contribution, and so, by suitable choice of test function η one will be able to make the 2nd variation negative. It follows that there are nearby solutions with lower energy, and we deduce that solutions of this kind are unstable.

Case (2): $\cos(ah + 2b) = 0$

In this case we have

$$\sin(ah + 2b) = \begin{cases} 1 & \text{case (2(i))} \\ -1 & \text{case (2(ii))} \end{cases}$$

so using (4.3) it is easily deduced that solutions a are given by the roots of

$$a = \begin{cases} \frac{\mathscr{A}}{2}\cos(ah) & \text{case (2(i))} \\ -\frac{\mathscr{A}}{2}\cos(ah) & \text{case (2(ii)).} \end{cases} \tag{4.8}$$

With these two cases allowed, we may assume $a > 0$ without loss of generality, since the $a < 0$ solutions in case (2(i)) are exactly equivalent to those $a > 0$ solutions in case (2(ii)). The corresponding solutions b satisfy

$$\text{Case (2(i)):} \quad \sin(ah + 2b) = 1 \Rightarrow \quad b = \tfrac{\pi}{4} - \tfrac{ah}{2} \quad (\text{modulo } \pi), \tag{4.9}$$

$$\text{Case (2(ii)):} \quad \sin(ah + 2b) = -1 \Rightarrow \quad b = \tfrac{3\pi}{4} - \tfrac{ah}{2} \quad (\text{modulo } \pi). \tag{4.10}$$

Then, considering the surface contributions to the 2nd variation, we have

$$\cos(2b) = \begin{cases} \sin(ah) & \text{case (2(i)),} \\ -\sin(ah) & \text{case (2(ii)),} \end{cases}$$

and

$$\cos(2ah + 2b) = \begin{cases} -\sin(ah) & \text{case (2(i)),} \\ \sin(ah) & \text{case (2(ii)).} \end{cases}$$

So, stability depends on the sign of $\sin(ah)$ in each case. For case (2(i)), $a = \mathscr{A}\cos(ah)/2$, if $\sin(ah) > 0$ then both surface contributions are positive, giving a net positive 2nd variation, and a stable solution. If $\sin(ah) < 0$ then both surface contributions to the 2nd variation (4.7) are negative, and thus the 2nd variation can be made negative for a suitable choice of η, so the solution is unstable. For case (2(ii)), $a = -\mathscr{A}\cos(ah)/2$, the reverse holds: if $\sin(ah) < 0$ then both surface contributions to the 2nd variation are positive, giving a net positive 2nd variation, and a stable solution, while if $\sin(ah) < 0$ then both surface contributions are negative, so the solution is unstable. Figure 3 illustrates the situation.

The solution observed in practice will be that stable solution of lowest energy, i.e. that with the lowest value of a, since ah represents the angle turned through by the director across the film. Thus, the observed solution will be the smallest stable root of

$$a = \frac{\mathscr{A}}{2}\cos ah \tag{4.11}$$

(case (2(i)), with b given by (4.9) (see Figure 3(a)); this solution always exists, whatever the value of $\mathscr{A}$), which lies in the range

$$0 < a < \frac{\pi}{2h}. \tag{4.12}$$

The free elastic energy W is again given by

$$W = \frac{\theta_z^2}{2} = \frac{a^2}{2}. \tag{4.13}$$

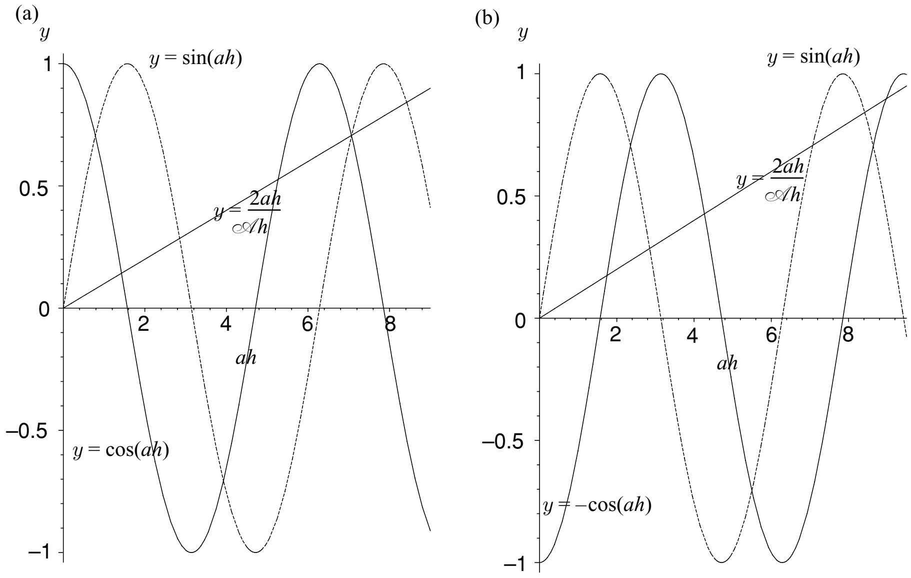

FIGURE 3. (a): Case (2(i)) $a = \mathscr{A}\cos(ah)/2$. Solutions a are given by the intersection of the solid curves $y = \cos(ah)$ and $y = 2(ah)/(\mathscr{A}h)$, and these are stable if the corresponding value of $\sin(ah)$ (the dotted curve) is positive. Thus, the first root is stable, the second unstable, the third stable, and so on, alternating between stable and unstable as a increases for as long as roots exist. (b): Case (2(ii)) $a = -\mathscr{A}\cos(ah)/2$. Solutions a are given by the intersection of the solid curves $y = -\cos(ah)$ and $y = 2(ah)/(\mathscr{A}h)$, and are stable if the corresponding value of $\sin(ah)$ (dotted) is negative. Thus, the first root is unstable, the second stable, the third unstable, and so on.

4.2 Momentum

We now return to the momentum equations to see how the analysis of § 3.2 is modified. Equations (3.17)–(3.20) are unchanged; but the different solution for θ means that the right-hand sides of the stress conditions (3.21) and (3.22) are altered, giving the modified stress boundary conditions

$$\begin{aligned}\frac{\partial u}{\partial z}&\big(2\alpha_1\sin^2\theta\cos^2\theta + (\alpha_5-\alpha_2)\cos^2\theta + (\alpha_3+\alpha_6)\sin^2\theta + 1\big)\\ &= -\mathscr{N}a(ha_x + b_x)\\ &= -\frac{\mathscr{N}a}{2}\big(ha_x - ah_x\big) \quad \text{on } z = h(x,y,t), \end{aligned} \tag{4.14}$$

$$\begin{aligned}\frac{\partial v}{\partial z}\big((\alpha_5-\alpha_2)\cos^2\theta + 1\big) &= -\mathscr{N}a(ha_y + b_y)\\ &= -\frac{\mathscr{N}a}{2}\big(ha_y - ah_y\big) \quad \text{on } z = h(x,y,t), \end{aligned} \tag{4.15}$$

where we have used (4.9) to eliminate b from the right-hand sides. Imposing no-slip at $z = 0$ and the kinematic condition at the free surface as before, we may again obtain a partial differential equation governing the evolution of the film height:

$$\frac{\partial h}{\partial t} + \frac{\partial}{\partial x}\left[\mathscr{J}_1\left(\mathscr{C}\left(\nabla^2 h\right)_x - \mathscr{B}h_x - \mathscr{N}aa_x\right) - \mathscr{J}_2\mathscr{N}a(ha_x - ah_x)\right] + \frac{\partial}{\partial y}\left[\mathscr{J}_3\left(\mathscr{C}\left(\nabla^2 h\right)_y - \mathscr{B}h_y - \mathscr{N}aa_y\right) - \mathscr{J}_4\mathscr{N}a(ha_y - ah_y)\right] = 0, \tag{4.16}$$

where a is determined by (4.11) and (4.12), and $\mathscr{J}_1$ to $\mathscr{J}_4$ are defined by

$$\mathscr{J}_1 = \frac{G_1(ah)}{a^3}, \quad \mathscr{J}_2 = \frac{G_2(ah)}{a^2}, \quad \mathscr{J}_3 = \frac{G_3(ah)}{a^3}, \quad \mathscr{J}_4 = \frac{G_4(ah)}{a^2}, \tag{4.17}$$

where

$$G_1(\lambda) = \frac{1}{4}\int_{\frac{\pi}{2}-\lambda}^{\frac{\pi}{2}+\lambda} \frac{(\pi/2 + \lambda - \xi)^2\, d\xi}{\alpha_1 \sin^2\xi + 2\eta_b(1 - \cos\xi) + 2\eta_c(1 + \cos\xi)} \tag{4.18}$$

$$G_2(\lambda) = \frac{1}{4}\int_{\frac{\pi}{2}-\lambda}^{\frac{\pi}{2}+\lambda} \frac{(\pi/2 + \lambda - \xi)\, d\xi}{\alpha_1 \sin^2\xi + 2\eta_b(1 - \cos\xi) + 2\eta_c(1 + \cos\xi)} \tag{4.19}$$

$$G_3(\lambda) = \frac{1}{4}\int_{\frac{\pi}{2}-\lambda}^{\frac{\pi}{2}+\lambda} \frac{(\pi/2 + \lambda - \xi)^2\, d\xi}{2\eta_c(1 + \cos\xi) + (1 - \cos\xi)} \tag{4.20}$$

$$G_4(\lambda) = \frac{1}{4}\int_{\frac{\pi}{2}-\lambda}^{\frac{\pi}{2}+\lambda} \frac{(\pi/2 + \lambda - \xi)\, d\xi}{2\eta_c(1 + \cos\xi) + (1 - \cos\xi)} \tag{4.21}$$

where the η_b, η_c are the Miesowicz viscosities defined in (3.26). The $G_i(\lambda)$ are plotted in Figure 4 for $0 < \lambda < \pi/2$ (this being the physically-relevant range, by (4.12)) for the α_i-values of MBBA at 25°C quoted in Kneppe *et al.* [6]. Again, they are always positive on the range of interest.

Again, if gravity instead acts parallel to the film then the governing equation analogous to (3.27) is easily written down:

$$\frac{\partial h}{\partial t} + \frac{\partial}{\partial x}\left[\mathscr{J}_1\left(\mathscr{C}\left(\nabla^2 h\right)_x - \mathscr{B}_1 - \mathscr{N}aa_x\right) - \mathscr{J}_2\mathscr{N}a(ha_x - ah_x)\right] + \frac{\partial}{\partial y}\left[\mathscr{J}_3\left(\mathscr{C}\left(\nabla^2 h\right)_y - \mathscr{N}aa_y\right) - \mathscr{J}_4\mathscr{N}a(ha_y - ah_y)\right] = 0. \tag{4.22}$$

4.3 Energy: Finite planar anchoring at substrate and finite homeotropic anchoring at free surface

If we reverse the anchoring conditions considered above, and instead assume that the liquid crystal molecules prefer to lie parallel to the rigid substrate, and perpendicular to the free surface, then the above analysis follows through almost unchanged. The surface energies now have the form

$$g_{\pm} = \text{constant} \mp \frac{\mathscr{A}_{\pm}}{2}\cos^2\theta, \tag{4.23}$$

the director solution is again given by (4.2), where, to satisfy the boundary conditions

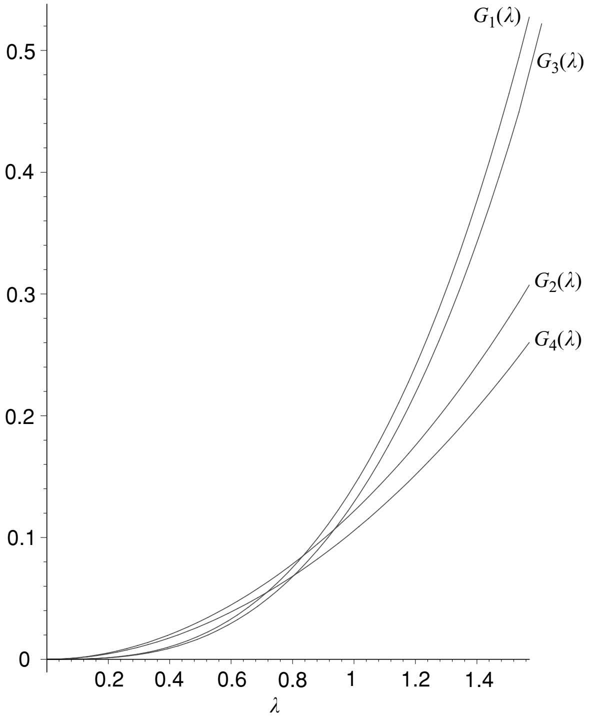

FIGURE 4. The functions $G_i(\lambda)$ for $0 < \lambda < \pi/2$, using the values for the viscosities α_i of MBBA at 25°C given in Table I of Kneppe *et al.* [6].

(3.9) at each interface a and b must satisfy

$$a = -\frac{\mathscr{A}_+}{2}\sin(2ah + 2b), \tag{4.24}$$

$$a = -\frac{\mathscr{A}_-}{2}\sin(2b). \tag{4.25}$$

Again, $a \equiv 0$, $b = 0, \pi/2$ are the only possible solutions with $a = 0$, and both are unstable. If we again assume $\mathscr{A}_+ = \mathscr{A}_- = \mathscr{A}$ then possible solutions must satisfy one of the possibilities (4.6). Stability of solutions is determined by the sign of the second variation, which here is

$$\begin{aligned}(\Delta J)_2 = \frac{\epsilon^2}{2}\iiint_\Omega \eta_z^2 dV + \frac{\mathscr{A}\epsilon^2}{2}\iint_{\partial\Omega^+}\eta^2\cos(2ah + 2b)dS \\ - \frac{\mathscr{A}\epsilon^2}{2}\iint_{\partial\Omega^-}\eta^2\cos(2b)dS.\end{aligned} \tag{4.26}$$

Case (1)

Here $ah = n\pi$, and so again $\cos(2ah + 2b) = \cos(2b)$. Hence as before there is always one positive and one negative contribution to the surface energy, and by suitable choice of the test function η the 2nd variation (4.26) may be made negative. These solutions are thus unstable.

Case (2)

We have two subcases

$$\sin(ah+2b)=\begin{cases}1 & \text{case } (2(\text{i}))\\ -1 & \text{case } (2(\text{ii})),\end{cases}$$

with $a>0$ without loss of generality; and correspondingly

$$\text{Case } (2(\text{i})):\quad b=\frac{\pi}{4}-\frac{ah}{2}\quad (\text{modulo } \pi), \tag{4.27}$$

$$\text{Case } (2(\text{ii})):\quad b=\frac{3\pi}{4}-\frac{ah}{2}\quad (\text{modulo } \pi). \tag{4.28}$$

Thus considering the terms in the 2nd variation (4.26),

$$\cos(2b)=\begin{cases}\sin(ah) & \text{case } (2(\text{i})),\\ -\sin(ah) & \text{case } (2(\text{ii})),\end{cases}$$

and

$$\cos(2ah+2b)=\begin{cases}-\sin(ah) & \text{case } (2(\text{i})),\\ \sin(ah) & \text{case } (2(\text{ii})),\end{cases}$$

so stability depends on the sign of $\sin(ah)$. For case (2(i)), $a=-\mathscr{A}\cos(ah)/2$, if $\sin(ah)>0$ then both surface contributions are negative and the solution is unstable, and if $\sin(ah)<0$ then both surface contributions are positive and the solution is stable. This is exactly equivalent to the case (2(ii)) considered in § 4.1 previously, and the situation is sketched in figure 3(b). (The director solution is not identical however, as the value of b differs in the two cases.)

For case (2(ii)), $a=\mathscr{A}\cos(ah)/2$, if $\sin(ah)<0$ then both surface contributions are negative and the solution is unstable, and if $\sin(ah)>0$ then both surface contributions are positive and the solution is stable. This is exactly equivalent to the case (2(i)) considered in § 4.1 previously, and the situation is sketched in Figure 3(a) (again though, the solution for b differs).

Hence the observed solution will be the smallest positive root of

$$a=\frac{\mathscr{A}}{2}\cos(ah), \tag{4.29}$$

with b given by (4.28). This director solution is exactly as in § 4.1 except for an additive term $\pi/2$. Thus the PDE governing the film height evolution follows almost exactly as before, with just minor changes to the definitions of the $\mathscr{J}_i$:

$$\begin{aligned}\frac{\partial h}{\partial t}&+\frac{\partial}{\partial x}[\mathscr{K}_1(\mathscr{C}(\nabla^2 h)_x-\mathscr{B}h_x-\mathscr{N}aa_x)-\mathscr{K}_2\mathscr{N}a(ha_x-ah_x)]\\ &+\frac{\partial}{\partial y}[\mathscr{K}_3(\mathscr{C}(\nabla^2 h)_y-\mathscr{B}h_y-\mathscr{N}aa_y)-\mathscr{K}_4\mathscr{N}a(ha_y-ah_y)]=0,\end{aligned} \tag{4.30}$$

where a is determined by (4.29), and $\mathscr{K}_1$ to $\mathscr{K}_4$ are defined by

$$\mathscr{K}_1=\frac{H_1(ah)}{a^3},\quad \mathscr{K}_2=\frac{H_2(ah)}{a^2},\quad \mathscr{K}_3=\frac{H_3(ah)}{a^3},\quad \mathscr{K}_4=\frac{H_4(ah)}{a^2}, \tag{4.31}$$

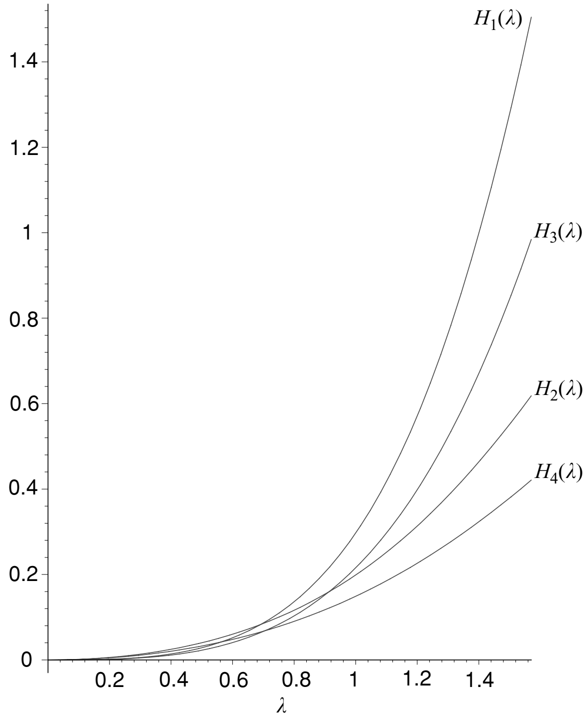

FIGURE 5. The functions $H_i(\lambda)$ for $0 < \lambda < \pi/2$, using the values for the viscosities α_i of MBBA at 25°C given in Table I of Kneppe *et al.* [6].

$$H_1(\lambda) = \frac{1}{4}\int_{\frac{\pi}{2}-\lambda}^{\frac{\pi}{2}+\lambda} \frac{(\pi/2+\lambda-\xi)^2\, d\xi}{\alpha_1 \sin^2\xi + 2\eta_b(1+\cos\xi) + 2\eta_c(1-\cos\xi)} \tag{4.32}$$

$$H_2(\lambda) = \frac{1}{4}\int_{\frac{\pi}{2}-\lambda}^{\frac{\pi}{2}+\lambda} \frac{(\pi/2+\lambda-\xi)\, d\xi}{\alpha_1 \sin^2\xi + 2\eta_b(1+\cos\xi) + 2\eta_c(1-\cos\xi)} \tag{4.33}$$

$$H_3(\lambda) = \frac{1}{4}\int_{\frac{\pi}{2}-\lambda}^{\frac{\pi}{2}+\lambda} \frac{(\pi/2+\lambda-\xi)^2\, d\xi}{2\eta_c(1-\cos\xi) + (1+\cos\xi)} \tag{4.34}$$

$$H_4(\lambda) = \frac{1}{4}\int_{\frac{\pi}{2}-\lambda}^{\frac{\pi}{2}+\lambda} \frac{(\pi/2+\lambda-\xi)\, d\xi}{2\eta_c(1-\cos\xi) + (1+\cos\xi)} \tag{4.35}$$

where the η_b, η_c are the Miesowicz viscosities defined in (3.26). The functions H_i are plotted in Figure 5.

4.4 Linear stability revisited

We again consider the linear stability of the simplest static solution to these two models (4.16) and (4.30): the uniform film $h = 1$. We write

$$h = 1 + \epsilon e^{\beta t} h_1(x, y) + O(\epsilon^2), \tag{4.36}$$

$$a = a_0 + \epsilon e^{\beta t} a_1(x, y) + O(\epsilon^2), \tag{4.37}$$

where to satisfy (4.11) (or (4.29)) we require

$$a_0 = \frac{\mathscr{A}}{2}\cos a_0, \qquad a_1 = -\frac{h_1 a_0\sqrt{\mathscr{A}^2 - 4a_0^2}}{2 + \sqrt{\mathscr{A}^2 - 4a_0^2}} = -\lambda_2 h_1 \tag{4.38}$$

(the inequality $\mathscr{A}^2 > 4a_0^2$ is satisfied automatically), where the second equality in the equation for a_1 defines the positive constant λ_2.

Substitution in (4.16) then gives the eigenvalue problem for h_1:

$$\begin{aligned}\beta h_1 &+ \frac{\partial}{\partial x}\left[\mathscr{J}_1\left(\mathscr{C}\left(\nabla^2 h_1\right)_x - \mathscr{B}h_{1x} + \mathscr{N}a_0\lambda_2 h_{1x}\right) + \mathscr{J}_2\mathscr{N}a_0(\lambda_2 + a_0)h_{1x}\right] \\ &+ \frac{\partial}{\partial y}\left[\mathscr{J}_3\left(\mathscr{C}\left(\nabla^2 h_1\right)_y - \mathscr{B}h_{1y} + \mathscr{N}a_0\lambda_2 h_{1y}\right) + \mathscr{J}_4\mathscr{N}a_0(\lambda_2 + a_0)h_{1y}\right] = 0,\end{aligned} \tag{4.39}$$

if we instead substitute in (4.22) then we simply replace $\mathscr{J}_i$ by $\mathscr{K}_i$ in the above. Bounded solutions to this problem are of the form $h_1 = \exp(ikx + iqy)$. Hence the eigenvalues $\beta(k, q)$ are given by

$$\beta = -[\mathscr{J}_1 k^2 + \mathscr{J}_3 q^2]\left(\mathscr{C}(k^2 + q^2) + \mathscr{B} - \mathscr{N}a_0\lambda_2\right) + [\mathscr{J}_2 k^2 + \mathscr{J}_4 q^2]\mathscr{N}a_0(\lambda_2 + a_0), \tag{4.40}$$

(or the equivalent expression with $\mathscr{K}_i$) and stability again depends on the relative values of $\mathscr{B}$ and $\mathscr{N}$, with instability if $\mathscr{N}$ is sufficiently large relative to $\mathscr{B}$.

4.5 Physical examples

We consider a film with the following physical characteristics:

- $\delta L =$ film thickness $= O(10^{-5})$m
- $L =$ horizontal extent of film, in range 10^{-3}–10^{-2}m
- Elastic constant $K = O(10^{-11})$N
- Anchoring energy A in range 10^{-6}–10^{-5} Jm^{-2} [10]
- Representative viscosity $\mu = 4 \times 10^{-2}$ Pa s (based on MBBA)
- Leslie viscosities α_i as for MBBA at 25°C [6]
- Density $\rho = 10^3$ kg m^{-3} (based on water).

Assuming a Bond number of unity, which fixes the velocity scale U, this gives approximate values for the remaining dimensionless parameters:

$$\mathscr{N} = O(1), \quad 1 < \mathscr{A} < 10, \quad \gamma < \mathscr{C} < \gamma 10^2, \tag{4.41}$$

where γ is the isotropic contribution to the surface tension. In the absence of accurate data for γ, if we assume it is not too different to that for an air-water interface, and take $\gamma = 0.1\,\mathrm{Nm}^{-1}$, then we obtain a range of values $0.1 < \mathscr{C} < 10$, the value $\mathscr{C} = 1$ corresponding to a film of horizontal extent $L \approx 3$ mm.

If we take $\mathscr{A} = 5$ then the value of a_0 as determined by (4.38) is $a_0 = 1.1105$, with $\lambda_2 = 0.7677$. The functions $\mathscr{J}_i$ can be easily evaluated at $h = 1$, $a = a_0$, and we find that

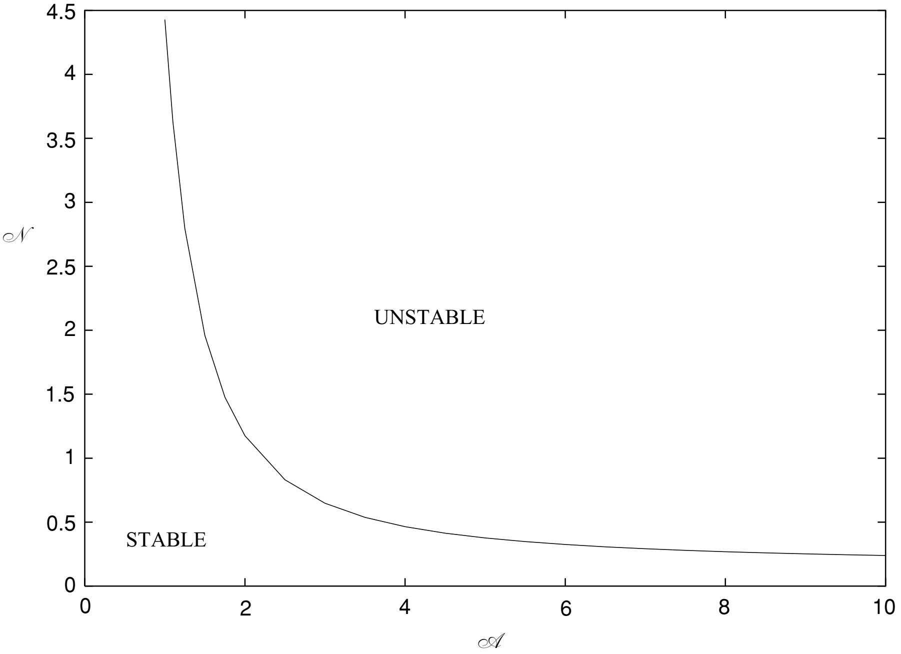

FIGURE 6. The stability curve for the solution $h = 1$ of (4.16), in $(\mathscr{A}, \mathscr{N})$-space, using the values for the viscosities α_i of MBBA at 25°C given in Table I of [6]. Here the instability is always via a k-mode.

the dispersion relation (4.40) becomes

$$\beta = -\mathscr{C}(k^2 + q^2)[0.141k^2 + 0.128q^2] - 0.374k^2[0.376 - \mathscr{N}] - 0.328q^2[0.388 - \mathscr{N}]. \quad (4.42)$$

Thus in this case we anticipate instability of the free surface if $\mathscr{N} > 0.376$ (a k-mode), which will likely be the case for the parameters quoted.

If we take $\mathscr{A} = 1$ then $a_0 = 0.45018$, with $\lambda_2 = 0.08044$. The $\mathscr{J}_i$ are again easily evaluated at $h = 1$, $a = a_0$, giving the dispersion relation (4.40) as

$$\beta = -\mathscr{C}(k^2 + q^2)[0.159k^2 + 0.140q^2] - 0.0359k^2[4.428 - \mathscr{N}] - 0.0313q^2[4.491 - \mathscr{N}]. \quad (4.43)$$

Thus in this case we anticipate instability of the free surface only if $\mathscr{N} > 4.428$, again via a k-mode.

More generally we may plot the curve of $\mathscr{N}_c$ as a function of $\mathscr{A}$, where $\mathscr{N}_c$ is the critical value of $\mathscr{N}$ at which instability sets in for the given value of $\mathscr{A}$ ($\mathscr{N} > \mathscr{N}_c$ corresponds to instability). Figure 6 gives the stability diagram for the solution $h \equiv 1$ of (4.16); solutions for which $(\mathscr{A}, \mathscr{N})$ lie above the curve are unstable, and those for which $(\mathscr{A}, \mathscr{N})$ lie below the curve are stable. Figure 7 gives the equivalent stability diagram for the solution $h \equiv 1$ of (4.30).

Again, the comments at the end of § 3.4.1 apply. In all cases, the boundary conditions require that the director bends through some finite angle across the film, which becomes

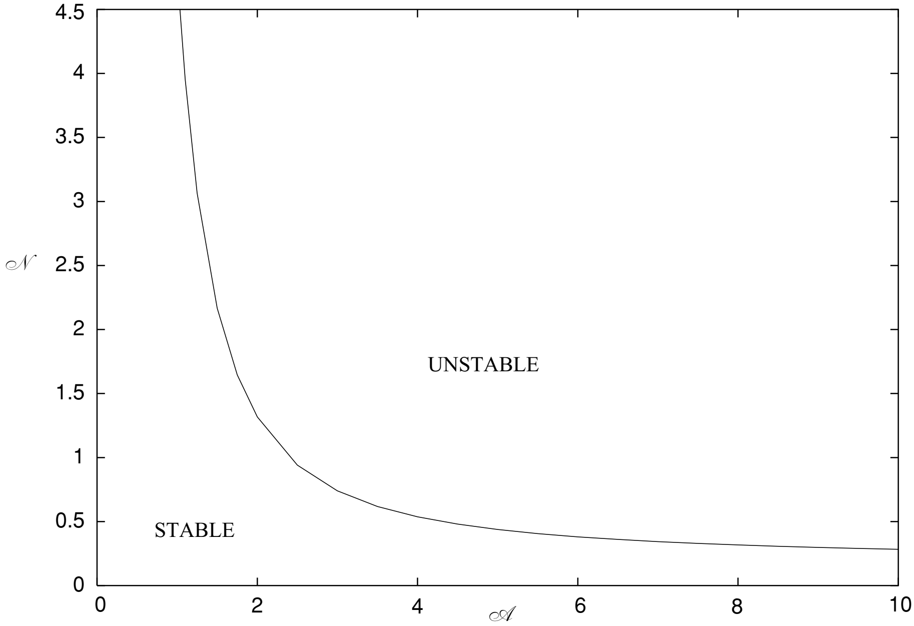

FIGURE 7. The stability curve for the solution $h = 1$ of (4.30), in $(\mathscr{A}, \mathscr{N})$-space, using the values for the viscosities α_i of MBBA at 25°C given in Table I of Kneppe *et al.* [6]. Here the instability is always via a q-mode.

more difficult to do as the film becomes thinner. The stronger the surface energy, the more firmly the director is anchored at either surface, and the more difficult its task of bending when the film is very thin. At some point it becomes energetically favourable for the free surface to destabilise. The smaller the value of the surface energy, the stabler the film, as the restrictions on the director at each surface are weaker. This is borne out by Figures 6 and 7, in each of which the stable region becomes smaller as $\mathscr{A}$ increases.

5 Can the film height go to zero?

An important question to consider is whether or not the film height can go to zero in the modified model of § 4. We know that neither the original model of Ben Amar & Cummings [1] (with strong anchoring at both surfaces) nor the model of § 3 (with strong anchoring at the substrate but weak (planar) anchoring at the free surface) admit solutions with $h \to 0$. To address this issue for the model with weak anchoring at both surfaces, we consider the 1-d version of (4.16).

As $h \to 0$ the value of a determined by (4.11) may be evaluated asymptotically; and we find

$$a = \frac{\mathscr{A}}{2} - \frac{\mathscr{A}^3 h^2}{16} + \cdots. \tag{5.1}$$

For small values of the argument λ the functions $G_1(\lambda)$ and $G_2(\lambda)$ may also be evaluated as

$$G_1(\lambda) = \frac{2\lambda^3}{3K} + \cdots \quad \Rightarrow \quad \mathscr{I}_1 = \frac{2h^3}{3K} + \cdots, \tag{5.2}$$

$$G_2(\lambda) = \frac{\lambda^2}{2K} + \cdots \quad \Rightarrow \quad \mathscr{I}_2 = \frac{h^2}{2K} + \cdots, \tag{5.3}$$

where $K = \alpha_1 + 2(\eta_b + \eta_c)$.

Thus, retaining the leading order terms in capillarity, gravity, and nematic effects, for small film heights h the 1-d version of (4.16) becomes

$$\frac{\partial h}{\partial t} + \frac{\partial}{\partial x}\left[\frac{2h^3}{3K}(\mathscr{C}h_{xxx} - \mathscr{B}h_x) + \frac{\mathscr{N}\mathscr{A}^2 h^2 h_x}{8K}\right] \approx 0, \tag{5.4}$$

in which clearly the term in $\mathscr{N}$ dominates the term in $\mathscr{B}$ as $h \to 0$. Hence, if static drop-like solutions (i.e. having compact support) to the full problem (3.27) are to exist, then locally they must satisfy

$$\frac{d}{dx}\left(h^3\frac{d^3h}{dx^3} + \frac{3\mathscr{N}\mathscr{A}^2}{16\mathscr{C}}h^2\frac{dh}{dx}\right) \approx 0. \tag{5.5}$$

Integrating this equation, assuming that h^3h''' and h^2h' ($' = d/dx$) both vanish as $h \to 0$ (thus we avoid the issue of a $\pi/2$ contact angle), we obtain

$$h\frac{d^3h}{dx^3} + \beta\frac{dh}{dx} = 0, \quad \text{where} \quad \beta = \frac{3\mathscr{N}\mathscr{A}^2}{16\mathscr{C}}$$

and, integrating twice more,

$$\left(\frac{dh}{dx}\right)^2 = -\beta h \log h + (k_1 + \beta)h + \tan^2\alpha, \tag{5.6}$$

where $\alpha > 0$ is the contact angle and k_1 is a constant of integration. If we take the positive square root for dh/dx (so that the contact line is to the left of the fluid domain), and fix constants such that the contact line is at $x = 0$, then the solution $h(x)$ is determined by

$$\int_0^h \frac{dH}{((k_1+\beta)H - \beta H\log H + \tan^2\alpha)^{1/2}} = x. \tag{5.7}$$

Clearly h cannot grow unboundedly from zero, as the term $-\beta h \log h$ dominates for large h, so that the right-hand side of (5.6) becomes negative, which is unacceptable. h grows until $dh/dx = 0$, which occurs when $h = h_*$, where

$$-\beta h_* \log h_* + (k_1 + \beta)h_* + \tan^2\alpha = 0.$$

This must happen at a finite value of x. If we had $h = h_*$ and $dh/dx = 0$ only at $x = \infty$, then the integral from $H = 0$ to $H = h^*$ in (5.7) must be divergent. This can happen only if the function $D(h) = (k_1 + \beta)H - \beta H \log H + \tan^2\alpha$ in the denominator of the integrand

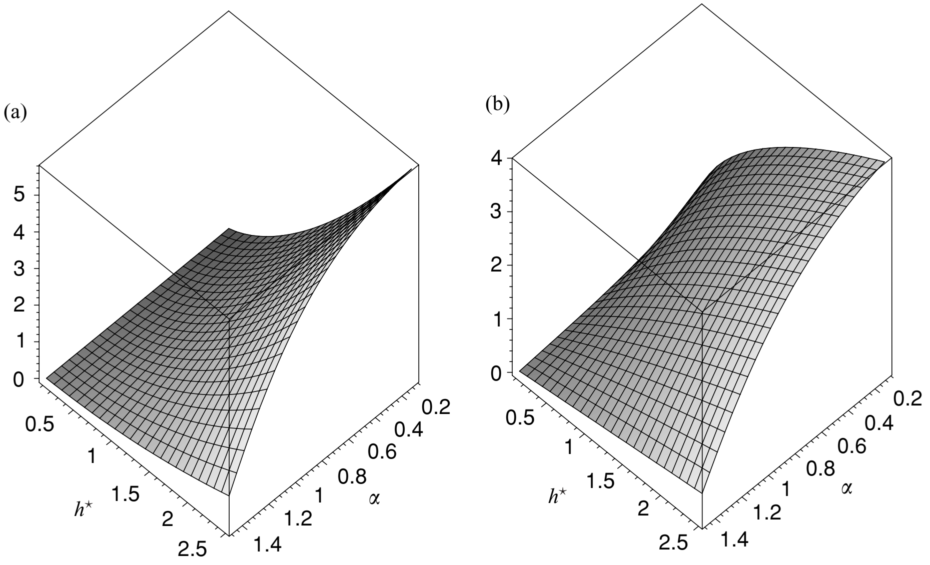

FIGURE 8. (a) The droplet half-volume $V/2$ as a function of contact angle α and droplet height h_* (the physical parameter β is taken to be 1). For each fixed α, V is a monotonic function of h_*, hence if V and α are specified, the corresponding h_* is uniquely determined. The droplet length x_* (plotted in (b) as a function of α and h_*) is then also uniquely determined.

has a repeated zero at $h = h_*$ (simple zeros, when square-rooted, are integrable). However, $D'(h) = 0$ only at $h_\dagger = \exp(k_1/\beta)$, and $D(h_\dagger) \neq 0$.

It follows that solutions starting from $h = 0$ inevitably increase to some finite value h_*, which is attained at some finite value $x = x_*$, at which there is a turning-point, and h must then decrease. Thus, for $x > x_*$ we must switch to the negative branch of the square-root, and the solution will again touch down at $x = 2x_*$. If the volume of the compactly-supported drop is $2V$ then

$$V = \int_0^{x_*} h\,dx = \int_0^{h_*} \frac{h}{dh/dx}\,dh = \int_0^{h_*} \frac{h\,dh}{(\beta\log(h_*/h) + (1 - h/h_*)\tan^2\alpha)^{1/2}} \tag{5.8}$$

which fixes the maximum drop height h_*, and its length $2x_*$ is determined by

$$x_* = \int_0^{h_*} \frac{dh}{(\beta\log(h_*/h) + (1 - h/h_*)\tan^2\alpha)^{1/2}} \tag{5.9}$$

(see figure 8). Plotting $V(\alpha, h_*)$ (Figure 8 (a)) we see that for a given volume $2V$ and contact angle α, the drop height h_* is uniquely determined, and hence so is the length, by (5.9) (Figure 8 (b)). Thus, there is a unique droplet solution of volume $2V$ and contact angle α, of height h_*, given by (5.7).

As an example, for $\beta = 1$, $\alpha = \pi/4$ and $V = 0.5$ we find $h_* = 0.689$, $x_* = 1.119$, and the corresponding solution h is shown in Figure 9.

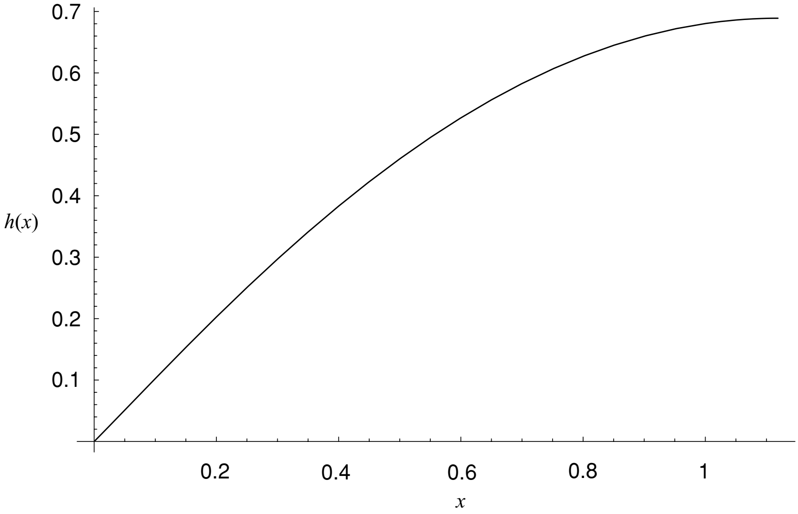

FIGURE 9. One half of a typical 'touchdown' solution to equation (5.5). The full profile is symmetric about the point x_* where the maximum height is attained.

6 Conclusions

We have used lubrication theory to derive a simple model governing the spreading (under gravity) of thin films of nematic liquid crystal, for various anchoring scenarios. This generalises the work of Ben Amar & Cummings [1], who considered only strong anchoring at both surfaces. The relevant partial differential equations governing the film height evolution were derived, and the stability of the simplest solution ($h \equiv 1$) to these PDEs was investigated. In all cases it was found that instability can occur, depending on the relative sizes of the Bond number, $\mathscr{B}$, and the inverse Ericksen number, $\mathscr{N}$. This suggests that, for sufficiently thin films, instability will be observed in practice. This fits with the experimental observations of Cazabat *et al.* [2], who observed spontaneous fingering instabilities in thin ($O(\mu$m)-thickness) spreading films of NLCs. Such instability can be understood physically by the fact that the different conditions imposed at the two interfaces (the anchoring on the NLC molecules) require the director to bend through some finite angle across the sample. The thinner the sample, the greater the energy penalty in doing this. At some critical film thickness, it becomes energetically favourable for the free surface to destabilise. The lower the surface anchoring energy, the stabler the situation, as is borne out by the stability plots of Figures 6 and 7.

In the case that our model is unstable, our results enable a most unstable wavelength to be easily identified, given all the relevant experimental parameter values (just solve $\partial\beta/\partial k = 0 = \partial\beta/\partial q$ for k and q to find the most unstable solution). It is hoped to be able to use this to make comparison with experimental data, once further experimental results are available.

We neglected the effect of Van der Waals' forces in this paper, thus, bearing in mind the upper limits on the film thickness given by (3.1), the model derived is valid for films of micron-level thickness. However, if thinner films are being modelled, the effect of such long-range intermolecular forces could easily be incorporated [12].

A numerical study of the film height evolution equations is underway, which should provide much greater insight into the possible behaviour of such thin nematic films, and which may also suggest possible new experimental investigations.

We finally considered briefly whether or not the models admit solutions in which the film height can go to zero, and found compactly-supported solutions for the simplified time-independent small-h equation; but the stability of these static solutions was not addressed. Neither was the case in which the contact angle is $\pi/2$ considered. Again, detailed numerical investigation of the equations will be of help.

Acknowledgements

The author acknowledges generous financial support from National Grid in the form of a Royal Society Dorothy Hodgkin Fellowship. She also thanks the referees for several helpful comments, and in particular, for drawing the reference [6] to her attention.

References

[1] Ben Amar, M. and Cummings, L. J. (2001) Fingering instabilities in driven thin nematic films. *Phys. Fluids*, **13**(5), 1160–1166.

[2] Cazabat, A.M., Valignat, M.-P., van Effenterre, D., Vandenbrouck, F. *Unpublished.*

[3] Chandrasekhar, S. (1992) Liquid Crystals (2nd ed). *Cambridge University Press.*

[4] De Gennes, P. G. and Prost, J. (1993) *The Physics of Liquid Crystals (2nd ed)*. International Series of Monographs on Physics (83), Oxford Science Publications.

[5] Joanny, J.-F. (1985) Le mouillage: quelques problemes statiques et dynamiques. *Thèse de doctorat d'etat ès sciences physiques*. Université Pierre et Marie Curie, Paris VI.

[6] Kneppe, H., Schneider, F. and Sharma, N. K. (1982) Rotational viscosity γ_1 of nematic liquid crystals. *J. Chem. Phys.* **77** (6), 3203–3208.

[7] Leslie, F. M. (1979) Theory of flow phenomena in liquid crystals. *Adv. Liquid Crystals*, **4**, 1–81.

[8] Myers, T. G. (1998) Thin films with high surface tension. *SIAM Rev.* **40** (3), 441–462.

[9] Rapini, A. and Papoular, M. (1969) *J. Phys. (Paris) Colloq.* **30**, C4, 54.

[10] Slavinec, M., Crawford, G. D., Kralj, S. and Zumer, S. (1997) Determination of the nematic alignment and anchoring strength at the curved nematic-air interface. *J. Appl. Phys.* **81** (5), 2153–2156.

[11] Valignat, M.-P., Villette, S., Li, J., Barberi, R., Bartolino, R., Dubois-Violette, E. and Cazabat, A. M. (1996) Wetting and anchoring of a nematic liquid crystal on a rough surface. *Phys. Rev. Lett.* **77**(10), 1994–1997.

[12] Vandenbrouck, F., Valignat, M.-P. and Cazabat, A. M. (1999) Thin nematic films: Metastability and spinodal dewetting. *Phys. Rev. Lett.* **82**(13), 2693–2697.